The preparation of Pb(II)-imprinted polymers by the combination of surface-imprinted method with sol–gel method for the removal of Pb(II)

Bo Zhu, Lingyu Zhou, Qi Zhang, Xiaodong Wang, Hongmei Jiang*, Aimin Lu

*College of Science, Nanjing Agricultural University, 1 Weigang, Nanjing 210095, China, Tel. 086-25-84396697,
Fax: 086-25-84395255; emails: jianghongmei@njau.edu.cn (H. Jiang), 23212105@njau.edu.cn (B. Zhu), zhouly@njau.edu.cn (L. Zhou),
23212111@njau.edu.cn (Q. Zhang), 23212202@njau.edu.cn (X. Wang), luaimin@njau.edu.cn (A. Lu)*

ABSTRACT

A rigid Pb(II)-imprinted polymers were synthesized by the combination of surface-imprinted method with sol–gel method using (3-mercaptopropyl) trimethoxysilane as a functional monomer, Pb(II) and hexadecyltrimethylammonium bromide as template ions and tetraethoxysilane as cross-linker and were used as adsorbents for the removal of Pb(II). The effect of molar ratio of cross-linker to functional monomer on the morphology and adsorption performance has been evaluated. The effects of pH, initial concentration and adsorption time on the adsorption performance of Pb(II) on both sorbents were investigated. The maximum adsorption capacity calculated from Langmuir isotherm was 68.03 mg g^{-1} and 17.13 mg g^{-1} for Pb(II)-IIP and Pb(II)-NIP, respectively. Kinetics studies showed that the adsorption process obeyed the pseudo-second-order kinetic model. The selective adsorption coefficient of Pb(II)-IIP for Pb(II)/Ni(II), Pb(II)/Cd(II), Pb(II)/Hg(II) and Pb(II)/Co(II) are 117.5, 1.42, 4.9 and 30.24, respectively. The spent Pb(II)-IIP could be reused at least five cycles, demonstrating its good practicability.

Keywords: Ion-imprinted polymer; Surface-imprinted method; Sol–gel method; Adsorption; Pb(II)

1. Introduction

It is widely known that heavy metal ions pollution has become one of the key problems of environmental pollution. As one of heavy metal ions, Pb(II) has a threat to the human body and the entire ecosystem. Currently, the main sources of Pb(II) include mining, printing, metal plating, textiles, acid batteries industries, fertilizer industry, paper and pulp industries [1,2]. The wastewater discharged from these industries is the root cause for Pb(II) entering into ecosystems. Compared with other pollutants, Pb(II) is non-biodegradable and tends to be accumulated in living tissues [3], which can cause various diseases and disorders in kidneys, liver, brain, reproductive system and central nervous system [4]. Thus, developing an effective method to remove Pb(II) from aqueous solution is particularly necessary.

Many methods have been adopted for the removal of Pb(II) including chemical precipitation [5], ion exchange [6], membrane separation [7,8], electrode deposition [9] and adsorption [10,11]. Among them, adsorption is regarded as the most attractive method in practical application due to its simple operation, superior efficiency and benign environment [12,13]. Therefore, exploring an efficient adsorbent is of vital importance for the widely application of adsorption in water treatment. In recent years, many sorbents have been investigated for the Pb(II) removal, such as mineral adsorbents [14,15], agriculture wastes [16–18], activated carbon [19], modified inorganic materials [20–23] and so on. However, these materials exhibit low selectivity, which limits their application.

Ion-imprinted polymer (IIP) absorbents can overcome this drawback very well, because they can provide a special recognition system for the target ions due to the imprinting process. Based on the memory effect toward the selected heavy ion, some characteristics of template ion can be carved in the polymer, such as the specificity of interaction between the ligands

* Corresponding author.

and the target ions and the size and shape of the target metal ions [24,25]. In addition, these IIP adsorbents are stable under a wide pH range, inexpensive, high mechanical strength and easy to prepare. The traditional preparation methods of IIP include bulk polymerization, emulsion polymerization and suspension polymerization [26,27]. When using absorbents fabricated by above methods, the kinetics of the sorption/desorption process are unfavorable because the template and ligands are totally embedded in the bulk polymer matrices and the mass transfer must take place through a comparatively long distance [28,29]. In order to dissolve the above shortcomings, surface-imprinting polymerization has obtained wide attention. When using surface ion-imprinted technique, it is often combined with sol–gel process, which can easily prepare a high cross-linking, better thermal stability and chemical stability material. The imprinted polymer layer is introduced onto the surface of substrates through hydrolysis and condensation of alkoxysilanes. A variety of substrates have been applied for preparing Pb(II)-imprinted materials, for example, TiO_2 [30], silica gel [31], mesoporous silica gel [32,33] and magnetic nanoparticles [34–37]. Another efficient surface-imprinted method is the reaction between template ion and functional monomers and co-condensation between functional monomers and silylation of silica precursors are processed at the same time to generate surface ionic-imprinted functionalized silica particles, which can be named as co-surface-imprinted method. To meet these requirements, functional monomers containing chelated groups usually are chosen as silylating reagents. Compared with the first method, the second is more convenient and time-saving. Up to now, there are only few works reporting the preparation of IIPs using the second surface method. During these studies, Tetraethoxysilane (TEOS) was selected as cross-linking agent, 3-iodopropyltrimethoxysilane [38], 3-thiocyanatopropyl-triethoxysilane [39] and 3-aminopropyltriethoxysilane [40–42] were used as functional monomers. In view of the strong affinity between Pb^{2+} and sulfhydryl group (–SH), mercaptopropyltrimethoxysilane (MPTMS) has been successfully employed as functional groups for the fabrication of Pb(II)-imprinted polymer using mesoporous silica [32] or silica-coated magnetic nanoparticles [34] as substrates. However, there is no report about the synthesis of Pb(II)-imprinted polymer using MPTMS as functional monomer by co-surface-imprinted method, which is more convenient during the preparation of the material.

In this study, we designed to synthesize Pb(II)-IIP using MPTMS as functional monomer, Pb(II) and CTAB as template, TEOS as cross-linker through the combination of surface-imprinted method with sol–gel method and apply them for the removal of Pb(II) using flame atomic absorption spectrometer (FAAS) as determination technique. After removing the templates, a great deal of cavities originated from Pb(II) and CTAB will be generated, which will offer a high surface area volume and adsorption capacity. Moreover, the effects of the ratio of TEOS to MPTMS on the morphology and adsorption performance of the imprinted material were examined in detail. The prepared materials were characterized by scanning electron microscope (SEM), Brunauer–Emmett–Teller (BET), Fourier transform infrared spectroscopy (FTIR) and energy disperse spectroscopy (EDS). The adsorption and desorption performance and the selectivity of the Pb(II)-IIP for Pb(II) were investigated. The isotherm and kinetics analysis for the Pb(II) adsorption on the Pb(II)-IIP were also studied in this work.

2. Experimental

2.1. Instrument

A Hitachi Z-2000 atomic absorption spectrometer (AAS) (Hitachi, Japan) was applied to determine lead concentrations. A Pb hollow cathode lamp (Hitachi, Japan) operated at 6.5 mA was employed as the radiation source. Measurements were performed in the integrated absorbance (peak area) mode at 283.3 nm using a spectral band width of 1.3 nm. The prepared materials were characterized by TENSOR27 FTIR (Bruker, Germany) in the region of 400–4,000 cm^{-1}. The size and morphology were analyzed by S-3400N II SEM (Hitachi, Japan). The element components were analyzed by S-3400N II EDS (Hitachi, Japan). The specific surface area and the pore volume of samples were measured by V-Sorb 2800P BET (Gold APP, Beijing, China).

The pH of the solution was measured by a Mettler-Toledo FE20 pH meter (Mettler-Toledo, Shanghai, China) supplied with a combined electrode. A KQ-500B ultrasonic bath (Kunshan Ultrasonic Instrument, Suzhou, China) was applied to speed up the adsorption process.

2.2. Material

Pb(II) stock solution of 1,000 mg L^{-1} was prepared by dissolving $Pb(NO_3)_2$ in deionized water. Pb(II) solutions of different concentrations were prepared by serial dilution of the stock solution using deionized water. Hexadecyltrimethylammonium bromide, (3-mercaptopropyl) trimethoxysilane, tetraethoxysilane, ethanol, HCl, NaOH, $Cd(NO_3)_2 \cdot 4H_2O$, $Ni(NO_3)_2 \cdot 6H_2O$, $Co(NO_3)_2 \cdot 6H_2O$ and $NH_3 \cdot H_2O$ used in this work were all of analytical grade and purchased from Aladdin's reagent network (Aladdin, Shanghai, China).

2.3. Preparation of Pb(II)-IIP and Pb(II)-NIP

Pb(II)-IIP was prepared according to the co-surface-imprinted method. In brief, 0.333 g $Pb(NO_3)_2$, 0.5 g CTAB, 0.5 mL MPTMS and 5 mL EtOH were dissolved in 10 mL deionized water and stirred homogeneously at room temperature for 1 h. Then, 2 mL TEOS as cross-linker and 1 mL 30% ammonia water were added dropwise into the obtained mixed solution under vigorous stirring. After 24 h, the temperature of the solution was raised to 90°C by oil bath for 12 h, keeping stirring. Finally, the precipitate was filtered from the solution and soaked with 4 mol L^{-1} of HCl for 24 h in order to remove the lead and CTAB in polymer until no Pb(II) was determined by FAAS. Then Pb(II)-IIP was washed with deionized water and NaOH until pH reached up to 7 and dried in a drying oven at 60°C for the subsequent study.

For comparison, Pb(II)-NIP was prepared simultaneously following the same procedures in the absence of Pb(II) template.

2.4. Adsorption experiment

All the adsorption studies were conducted in batch modes. Briefly, a certain Pb(II)-IIP or Pb(II)-NIP were dispersed into 10 mL of sample solution with the chosen pH and the initial concentration of Pb(II). pH adjustments were

obtained with NH₃·H₂O and HCl. And then the mixture was blended together and immersed into an ultrasonic bath performed at 40 kHz of ultrasound frequency and 100 W of power to accelerate adsorption progress for an appropriate time. Afterwards, the adsorbent was deposited by centrifugation (4,000 rpm, 10 min) and the supernatant liquid was collected for the determination of Pb(II) by FAAS.

The effect of initial pH on the removal percentage of Pb(II) was evaluated at a pH ranges from 2 to 7. The adsorption studies were also examined as function of metal ions concentration (1–150 mg L⁻¹) and contact time (1–80 min). All experiments were run in duplicate and the average values were reported here. The removal percentage (*R*%) and adsorption capacity of Pb was calculated using by following equations:

$$R\% = (C_o − C_e)/C_o × 100\% \tag{1}$$

$$Q = (C_o − C_e)V/M \tag{2}$$

where C_o and C_e are concentrations of Pb (mg L⁻¹) in the solution before and after adsorption, respectively; where Q is the adsorption capacity (mg g⁻¹), V is the volume of metal ion solution (L) and W is the weight of the adsorbent (g).

2.5. Adsorption selectivity

In order to evaluate the selectivity of the sorbent for Pb(II), recognition studies of the competitive metal ions (Ni(II), Co(II), Hg(II) and Cd(II)) were performed. In the experiments, 20 mg Pb(II)-IIP or Pb(II)-NIP was mixed with 10 mL of sample solution containing Pb(II)/Ni(II), Pb(II)/Co(II), Pb(II)/Hg(II) or Pb(II)/Cd(II) with the concentration of 10 mg L⁻¹ in each case with pH 6. After reaching adsorption equilibrium, the concentrations of Pb(II), Ni(II), Co(II), Hg(II) and Cd(II) in solution were determined by FAAS. The distribution coefficient K_d, selectivity coefficient k, and the relative selectivity coefficient k' are given in Eqs. (3)–(5).

$$K_d = (C_o − C_e)V/C_e\, m \tag{3}$$

$$k = K_{d(1)}/K_{d(2)} \tag{4}$$

$$k' = K_{IIP}/K_{NIP} \tag{5}$$

where C_o and C_e are the concentrations of ions (mg L⁻¹) in the solution before and after adsorption, respectively; V is the volume of metal ions solution (L) and m is the weight of the adsorbent (g); $K_{d(1)}$ represents the distribution coefficient of Pb(II) and $K_{d(2)}$ represents the distribution coefficient of Ni(II), Co(II) and Cd(II). k_{IIP} and k_{NIP} represent the selectivity coefficient of Pb(II)-IIP and Pb(II)-NIP, respectively. And k' is the relative selectivity coefficient.

2.6. Desorption and regeneration experiments

The desorption and regeneration experiments were conducted as following: 20 mg Pb(II)-IIP was immersed in 10 mL of the sample solution containing 10 mg L⁻¹ concentration of Pb(II). After reaching adsorption equilibrium, the desorption was carried out by means of eluting the adsorbents with 0.5 mol L⁻¹ HCl solution. This adsorption–desorption procedures were run five times under equal conditions and the final Pb(II) concentration in the solution was determined by FAAS.

3. Results and discussion

3.1. Preparation and characterization of the materials

3.1.1. Effect of molar ratio of TEOS to MPTMS on the morphology and adsorption performance

The molar ratio of TEOS to MPTMS has a vast influence on the morphology and adsorption performance of Pb(II)-IIP as it decides the amount of functional sites and the weight of the silica matrix. The performance and the surface morphology of Pb(II)-IIP that was fabricated with various molar ratios of TEOS to MPTMS were studied and the results are shown in Table 1 and Fig. 1. As can be seen, when the ratio of TEOS/MPTMS was lower than 1, the product was hardened and formed a monoblock with many pores, which was because too little cross-linker could not offer sufficient silica matrix to produce network structure. After the ratio of TEOS/MPTMS was higher than 1, regular spherical particles with the mean particle size of 200 nm were generated and the adsorption capacity of Pb(II) was decreased with the increasing of the ratio. The dropped adsorption capacity was due to the declined functional groups provided by MPTMS, which was agreed well with the Wu et al. [43]. Hence, a ratio of 1.6 was selected to synthesize the material.

Table 1
The molar ratio of TEOS to MPTMS on the adsorption performance of Pb(II)

Sample	A	B	C	D
$M_{(TEOS/MPTMS)}$	5	3.3	1.6	0.9
Adsorption capability (mg g⁻¹)	6.92	7.9	10.72	–

ᵃPb(II): 0.333 g; CTAB: 0.5 g; deionized water: 10 mL; EtOH: 5 mL; NH₃·H₂O: 1 mL.
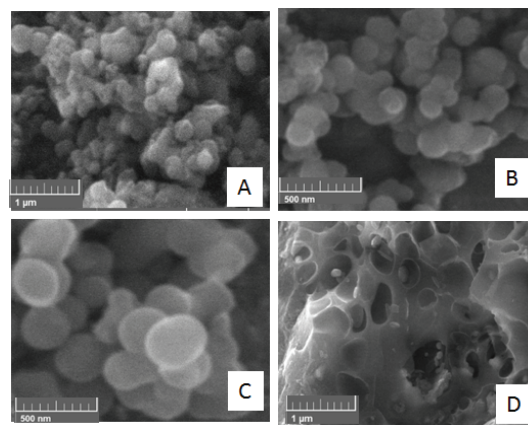

Fig. 1. SEM images of Pb(II)-IIP: (A) $M_{(TEOS/MPTMS)}$ = 5, (B) $M_{(TEOS/MPTMS)}$ = 3, (C) $M_{(TEOS/MPTMS)}$ = 1.6 and (D) $M_{(TEOS/MPTMS)}$ = 0.9.

3.1.2. FTIR spectrum

The FTIR technique is an important method to identify the characteristic functional groups that can produce strong affinity towards the metal ions. As it could be seen the similar main peaks in the FTIR spectra of both Pb(II)-IIP and Pb(II)-NIP exhibited in Fig. 2 not only suggested the similar polymeric backbones but also indicated that the leaching process did not affect the polymeric network [44,45]. The adsorption peak at 1,081 cm⁻¹ discovered on Pb(II)-IIP and Pb(II)-NIP was assigned to Si–O stretching vibration, reflecting the formation of a layer of silica on the surface of materials. In addition, the peak at 2,928 cm⁻¹ was ascribed to –CH$_3$ group from MPTMS and TEOS. The absorption peak of –SH group was not discovered in both spectra of Pb(II)-IIP and Pb(II)-NIP, which may be attributed to relatively lower content of –SH group.

3.1.3. EDS analysis

In order to verify the existence of –SH and the main composites of the Pb(II)-IIP and Pb(II)-NIP, EDS analysis was employed and the results are listed in Table 2. As revealed in Table 2, the main elements in both materials were C, O, Si and S and the contents of –SH in Pb(II)-IIP were higher than that in Pb(II)-NIP, contributing to a larger adsorption capacity of Pb(II). These results demonstrated that the imprinted polymer has been successfully formed.

3.1.4. BET analysis

Large specific surface area is one of the most important properties of porous adsorption materials. The specific surface area of Pb(II)-IIP and Pb(II)-NIP was determined by BET analysis illustrated in Table 3. The specific surface area of Pb(II)-IIP was found to be 394.40 m² g⁻¹, which was much higher than that of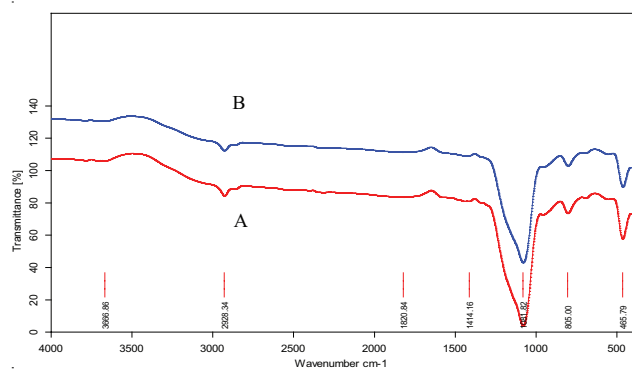 Pb(II)-NIP (50.98 m² g⁻¹). Meanwhile, the pore size of Pb(II)-IIP was measured as 3.42 nm, which was lower than that of Pb(II)-NIP (9.72 nm). The pore volume of Pb(II)-IIP and Pb(II)-NIP was found to be 0.37 and 0.14 cm³ g⁻¹, respectively. Compared with Pb(II)-NIP, the much larger surface area of Pb(II)-IIP was due to more cavities produced during the imprinted process, which would result in the higher adsorption capacity.

3.2. Adsorption experiments

3.2.1. Effect of pH

The pH has a significant effect on the uptake of metal ions, since it decides the existing species of metal ions and the ionization form of the functional groups on the surface of the adsorbent which will affect the availability of binding sites. The effects of pH on the removal percentage of Pb(II) by Pb(II)-IIP and Pb(II)-NIP were examined at pH range of 2–7. The results presented in Fig. 3 shows that the removal percentage of Pb(II) on both materials increased with the increasing of pH during the whole pH range. However, the removal percentage of Pb(II) on Pb(II)-IIP was much higher than that on Pb(II)-NIP and the removal percentage of Pb(II) on Pb(II)-IIP could reach 100% during the pH range from 6 to 7 while the

Table 3
BET analysis of Pb(II)-IIP and Pb(II)-NIP

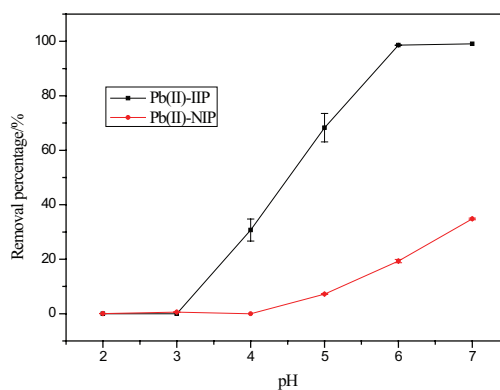| Sorbent	Specific surface (m² g⁻¹)	Pore volume (cm³ g⁻¹)	Average pore diameter (nm)
IIP	394.40	0.37	3.42
NIP	50.98	0.14	9.72

Fig. 3. Effects of pH on the removal of Pb(II) by Pb(II)-IIP and Pb(II)-NIP. C_{Pb}: 10 mg·L⁻¹; contact time: 30 min, dosage of adsorbent: 5 mg.

Fig. 2. FTIR spectrum of Pb(II)-IIP (A) and Pb(II)-NIP (B).

Table 2
EDS analysis of Pb(II)-IIP and Pb(II)-NIP

Material	C		O		Si		S	
	Weight %	Atomic %	Weight %	Atomic %	Weight %	Atomic %	Weight %	Atomic %
IIP	32.42	43.78	40.43	40.98	18.49	10.68	6.17	3.12
NIP	34.27	46.00	38.60	38.89	21.14	12.13	5.34	2.68

highest removal percentage of Pb(II) on Pb(II)-NIP was only about 20%. The effect of pH higher than 7 on the adsorption of Pb(II) on both materials was not investigated due to the easy formation of precipitation of hydroxide. When pH < 3, Pb(II) was nearly not reserved on both materials, which was because the active sites on the surface of Pb(II)-IIP and Pb(II)-NIP were positive in acidic solution due to the protonation and thus Pb(II) was repulsed by the materials. With the increasing of pH, the degree of the protonation decreased, electrostatic repulsion declined and the adsorption of Pb(II) on the sorbents enhanced. Besides, with the increase of pH, more and more chelate complex of Pb(II) and –SH was formed, especially after pH was up to 6. Because when we carried out the experiments, we found that Pb(II)-IIP material was white after eluting Pb(II) and they changed into yellow while adding Pb(II) solution. In other words, the materials were yellow if the chelate was formed and they were white when the chelate was destroyed. However, there was no any color change in the pH range of 2–3, which was due to nearly no absorption of Pb(II). The color change was strengthened with the increasing of pH and was the most obvious after pH value was arrived to 6, further confirming the speculation of the formation of chelate complex. Considering the removal efficiency and practicality, pH 6 was chosen as the optimum solution pH in the following studies.

3.2.2. Effect of initial metal concentration

The study about different initial metal ion concentration is quite important in optimizing their use in aqueous solution. The effect of initial metal ion concentration on the adsorption capacity of Pb(II) was analyzed in the range of 0–150 mg L^{-1} of Pb(II) and the results are shown in Fig. 4. It is evident from Fig. 4 that the uptake capacity improved rapidly with the increase of initial Pb(II) concentration and then attained a saturation value at 100 mg L^{-1} with a maximum equilibrium uptake for Pb(II) of 73 mg g^{-1} for Pb(II)-IIP adsorbent and 20 mg g^{-1} for Pb(II)-NIP adsorbent, respectively. The rapid adsorption during lower initial concentration was attributed to the availability of numerous active sites on the surface of the adsorbents. While with the improving concentration, more Pb(II) remained unabsorbed because the binding sites were occupied. Hence, the experimental value of maximum adsorption capacity was 73 mg g^{-1}.
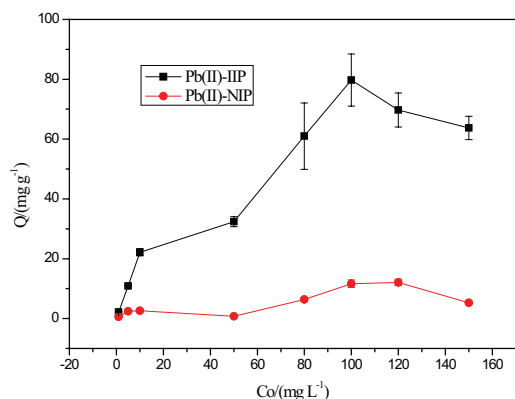

Fig. 4. Effects of initial Pb(II) concentration on the adsorption capacity of Pb(II) on Pb(II)-IIP and Pb(II)-NIP. pH: 6; contact time: 30 min, dosage of adsorbent: 5 mg.

3.2.3. Effect of contact time

The contact time between the adsorbate and adsorbent is another very important parameter for the adsorption of metal ions. The effects of contact time on the adsorption capacity of Pb(II) on both Pb(II)-IIP and Pb(II)-NIP were investigated in this study and the results are shown in Fig. 5. As Fig. 5 demonstrates, the adsorption of Pb(II) on Pb(II)-IIP and Pb(II)-NIP with an initial Pb(II) concentrations of 100 mg L^{-1} was very fast and the equilibrium was established after 40 and 5 min, respectively. To 100 mg L^{-1} Pb(II), it just needed 40 min to achieve adsorption equilibrium, which revealed that Pb(II) were very easy to enter into a great deal of imprinted cavities and bound with the recognition sites on the surface of Pb(II)-IIP. Compared with Pb(II)-IIP, less active sites and cavities generated in the Pb(II)-NIP contributed to the faster adsorption rate of Pb(II), needing only 5 min to obtain adsorption equilibrium. Moreover, the maximum adsorption of Pb(II) on Pb(II)-IIP was about 70 mg g^{-1}, much larger than that on Pb(II)-NIP (about 20 mg g^{-1}). This phenomenon could be explained as the available active sites and cavities on the surface of Pb(II)-IIP, produced in the imprinted process, were much more than that of Pb(II)-NIP, which further confirmed the above speculation.

3.2.4. Adsorption kinetics

To evaluate the reaction pathways of adsorption processes such as mass transfer, diffusion control and chemical reaction, the kinetic datum obtained from batch experiments were fitted pseudo-second-order rate equation, which was a classic kinetic model and could be expressed as the following form:

$$\frac{t}{q_t} = \frac{1}{k_2 q_e^2} + \frac{t}{q_e} \tag{6}$$

where q_t (mg g^{-1}) was the amount of adsorption at time t (min), k_2 (g (mg min)$^{-1}$) was the rate constant of the pseudo-second-order kinetic adsorption as well as q_e was the equilibrium adsorption capacity.
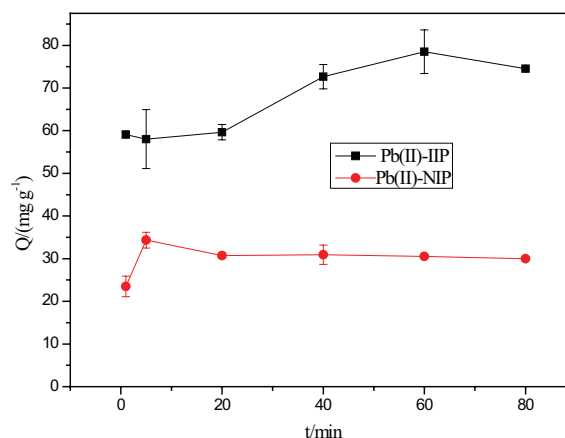

Fig. 5. Effects of contact time on the adsorption capacity of Pb(II) on Pb(II)-IIP and Pb(II)-NIP. C_{Pb}: 100 mg·L^{-1}; pH: 6; dosage of adsorbent: 5 mg.

The values of q_e and k_2 could be obtained from the slopes and intercepts of the linear curve of t/q_t vs. t and are showed in Table 4. As demonstrated in Table 4, the pseudo-second-order equation fitted well to the experimental datum of the Pb(II)-IIP and Pb(II)-NIP with a high correlation coefficients (R^2) of 0.99 for both sorbents. The theoretical q_e values calculated from the pseudo-second-order kinetic model, 71.38 and 25.5 mg g^{-1} for Pb(II)-IIP and Pb(II)-NIP, respectively, were also very close to the experimental values of 70 mg g^{-1} for Pb(II)-IIP and 20 mg g^{-1} for Pb(II)-NIP. These results suggested that the pseudo-second-order mechanism was predominant for the description of the Pb(II) adsorption on Pb(II)-IIP and Pb(II)-NIP and that chemical sorption may be the rate-limiting step that controlled the adsorption process.

3.2.5. Adsorption isotherm

The study on the adsorption isotherms was of great sense to describe the relationship between adsorbent and metal ions and it could help understand the adsorption mechanism.

The Langmuir adsorption isotherm was used in this work and could be expressed by following equation:

$$\frac{C_e}{q_e} = \frac{C_e}{q_m} + \frac{1}{q_m K_L} \tag{7}$$

where c_e (mg L^{-1}) is the equilibrium concentration in the solution, q_e (mg g^{-1}) is the adsorption capacity, q_m (mg g^{-1}) is the maximum binding capacity and K_L (L mg^{-1}) is the equilibrium constant.

Linear plots of c_e/q_e vs. c_e were employed to determine the value of q_{max} and K_L and the results are listed in Table 4. As shown in Table 4, the calculated Langmuir constant q_{max} were 68.03 and 17.13 mg g^{-1} for Pb(II)-IIP and Pb(II)-NIP, respectively, which were in good agreement with the respective experimental q_{max} values, indicating that the sorption sites are basically homogeneous. Besides, a comparison of absorption capacity of Pb(II) on different imprinted adsorbents is demonstrated in Table 5. It can be seen that the material

Table 4
Langmuir parameters and kinetic parameters for the adsorption of Pb(II) on Pb(II)-IIP and Pb(II)-NIP

Material	Langmuir parameters			Pseudo-second-order parameters		
	q_{max} (mg g^{-1})	k_L (L mg^{-1})	R^2	q_e (mg g^{-1})	k_2 (g (mg min)$^{-1}$)	R^2
Pb(II)-IIP	68.03	0.5282	0.98	71.38	0.0057	0.99
Pb(II)-NIP	17.13	2.2662	0.95	25.5	0.0112	0.99

Table 5
Comparison of adsorption capacity of Pb(II) on different ion-imprinted polymer

Absorbents	Functional monomer	Cross-linker	Absorption capacity (mg·g^{-1})	Reference
Pb(II)-imprinted polymer in nano-TiO$_2$ matrix	Chitosan	Glycidoxypropyltrimethoxysilane	22.7	30
Pb(II)-imprinted amino-functionalized silica gel sorbent	3-Aminopropyltrimethoxysilane	Activated silica	19.66	31
Pb(II)-IIP using CTS as functional monomer on support matrix of SBA-15	Chitosan	γ-(2,3-epoxypropo-xy) propyltrimethoxysilane	42.55	33
Magnetic ion-imprinted polymer (Fe$_3$O$_4$@SiO$_2$-IIP)	3-Mercaptopropyl trimethoxysilane	Tetraethyl orthosilicate	32.58	34
Pb(II) ion–imprinted polymer coated on magnetic mesoporous silica	Allyltrimethoxysilane	Tetraethyl orthosilicate	68.1	36
Magnetic ion–imprinted polymer (IIP)	4-(vinylamino) pyridine-2,6-dicarboxylicacid	Ethylene glycol dimethacrylate 2,2'-Azo bis isobutyro nitrile	55.89	37
Pb(II)-ion-imprinted silica-supported organic–inorganic hybrid	Chelating Schiff base ligands derived from the 3-aminopropyltrimeth-oxysilane and 2-thiophenecarboxalde-hyde	Tetraethoxysilicate	54.9	40
Pb(II)-imprinted polymers	(3-mercaptopropyl)-tri-methoxysilane	Tetraethoxysilane	68.03	This work

prepared in this work had a relatively higher absorption capacity than most other materials, which illustrated the effectiveness of preparation.

3.3. Thermodynamic study

In order to obtain the information about the inherent energetic changes associated with the adsorption, the thermodynamic study was examined in this work. The change in Gibbs free energy ($\Delta G°$, kJ mol^{-1}), enthalpy ($\Delta H°$, kJ mol^{-1}) and entropy ($\Delta S°$, J mol^{-1} K) of the adsorption process can be calculated from:

$$\Delta G° = -RT\ln K_d \tag{8}$$

$$\ln K_d = \frac{\Delta S°}{R} - \frac{\Delta H°}{RT} \tag{9}$$

where K_d is the equilibrium constant, which can be estimated using the method of Lyubchik et al. [46] by plotting $\ln(q_e/c_e)$ vs. q_e under different temperatures, R is the universal gas constant (8.314 J mol^{-1} K^{-1}) and T is the absolute temperature (K). $\Delta H°$ and $\Delta S°$ can be determined from the intercept and slope of the plot between $\ln K_d$ vs. $1/T$ and all thermodynamic parameters are listed in Table 6.

The negative value of ΔG suggested the spontaneity of the adsorption and the positive value of ΔH indicated the endothermic nature of adsorption, which was in agreement with the increase in adsorption capacity with increasing temperature. The positive value of ΔS demonstrated the increasing disorder at the solid–liquid interface during the adsorption of Pb(II) on Pb(II)-IIP, which was mainly due to the interaction of Pb(II) with the active binding sites of the adsorbents.

3.4. Adsorption selectivity

To examine the selectivity of the Pb(II)-IIP, Ni(II), Cd(II), Hg(II) and Co(II) were chosen as a comparative ions because they had the same charge and also can bind well with the ligand. For comparison, the selective adsorption was also carried out by using Pb(II)-NIP and the results are shown in Table 7. As seen in Table 7, under the presence of competitive ions, the distribution ratio K_d(Pb) and the selective adsorption coefficient k of Pb(II)-IIP was significantly higher than that of Pb(II)-NIP, indicating that Pb(II)-IIP had high affinity and selectivity of Pb(II). These results could be due to the imprinting process of Pb(II)-IIP material preparation. Pb(II)-IIP materials had specific cavities, which contained binding sites with functional ligands and constant size to match Pb(II). Moreover, these cavities and sites were in an orderly stereochemical arrangement. However, other ions and the imprinting cavities could not be able to complement each other, resulting in that the specific cavities could only adsorb Pb(II) preferentially. Additionally, the functional ligands of the non-imprinted adsorbent arranged randomly and disorderly and more importantly there were no imprinted cavities in Pb(II)-NIP, bringing about unremarkable selectivity performance.

Table 6
Thermodynamic parameters of Pb(II) adsorbed onto Pb(II)-IIP

T/K	Q_e (mg g^{-1})	$\Delta G°$ (kJ mol^{-1})	$\Delta H°$ (kJ mol^{-1})	$\Delta S°$ (J mol^{-1} K)
298	32	−6.52	1.83	32.26
308	39.9	−8.92		
318	70.7	−10.58		

Table 7
Selectivity parameters of Pb(II)-IIP and Pb(II)-NIP for Pb(II)

Metal ions	Sorbent	K_d(Pb)	K_d(M^a)	k	k'
Pb(II)/Co(II)	IIP	37,420	9	4158	30.24
	NIP	110	0.8	137.5	
Pb(II)/Cd(II)	IIP	6,670	1330	5.01	1.42
	NIP	53	15	3.53	
Pb(II)/Ni(II)	IIP	49,000	103	475.7	117.5
	NIP	81	20	4.05	
Pb(II)/Hg(II)	IIP	185	1117	0.17	4.9
	NIP	30	867	0.035	

Conditions: $m_{(Pb\text{-}IIP)}$ = 20 mg, $m_{(Pb\text{-}NIP)}$ = 20 mg, $C_{o(Pb)}$ = 10 mg·L^{-1}, $C_{o(M)}$ = 10 mg·L^{-1}, pH = 6, T = 30 min, V = 10 mL.
[a]M stands for the Co, Cd, Ni and Hg.

3.5. Desorption and regeneration

Regeneration allows for the reuse of the sorbent and is one of key factors for reducing costs in practical application. For repeated use of an adsorbent, adsorbed metal ions should be easily desorbed under proper conditions. The pH study displayed that Pb (II) was nearly not reserved by Pb(II)-IIP when pH < 3, implying that acid treatment is a feasible approach to regenerating the Pb (II). Hence, the desorption of the adsorbed Pb(II) by different concentrations of hydrochloric acid was investigated and the results showed that 0.5 mol L^{-1} HCl could desorb Pb(II) from the material. In order to examine the reusability of Pb(II)-IIP adsorbent, the adsorption/ desorption cycles were repeated several times and the results disclosed that the Pb(II)-IIP materials were still with the same adsorption capacity even after the fifth cycle. These results suggest that Pb(II)-IIP is with good reusability and selectivity and has a great potential in practical application.

4. Conclusions

In this study, a new Pb(II)-IIP using MPTMS as functional monomer, Pb(II) and CTAB as template, TEOS as cross-linker have been fabricated through the combination of surface-imprinted method with sol–gel method and applied them for the removal of Pb(II). Moreover, we found that the molar ratio of TEOS to MPTMS in the preparation progress has a vast influence on the morphology and adsorption performance of Pb(II)-IIP. Proper molar ratio of TEOS to MPTMS could help to form a network of pore channels and regular spherical particles that could contribute to large surface areas and excellent transfer kinetics for metal ions. In comparison with Pb(II)-NIP, Pb(II)-IIP had higher adsorption capacities and higher selectivity for Pb(II), which was due to plenty

of active binding sites stemmed from MPTMS and cavities provided by Pb(II) and CTAB during the imprinted process. The absorbed Pb(II) could be desorbed by 0.5 mol L^{-1} HCl and Pb(II)-IIP could be reused five cycles without notable loss of adsorption performance, displaying good reusability and great potential for practical application.

Conflict of interest

The authors declare no conflict of interest.

References

[1] Z. Reddad, C. Gérente, Y. Andres, J. Thibault, P. Le Cloirec, Cadmium and lead adsorption by a natural polysaccharide in MF membrane reactor: experimental analysis and modeling, Water Res., 37 (2003) 3983–3991.

[2] B. Hui, Y. Zhang, L. Ye, Structure of PVA/gelatin hydrogel beads and adsorption mechanism for advanced Pb(II) removal, J. Ind. Eng. Chem., 21 (2015) 868–876.

[3] B.J. Liu, X. Lv, X.H. Meng, G.L. Yu, D.F. Wang, Removal of Pb(II) from aqueous solution using dithiocarbamate modified chitosan beads with Pb(II) as imprinted ions, Chem. Eng. J., 220 (2013) 412–419.

[4] T. Alizadeh, S. Amjadi, Preparation of nano-sized Pb^{2+} imprinted polymer and its application as the chemical interface of an electrochemical sensor for toxic lead determination in different real samples, J. Hazard. Mater., 190 (2011) 451–459.

[5] S. Mauchauffée, E. Meux, Use of sodium decanoate for selective precipitation of metals contained in industrial wastewater, Chemosphere, 69 (2007) 763–768.

[6] J.F. de Sá S. Costa, V.J.P. Vilar, C.M.S. Botelho, E.A.B. da Silva, R.A.R. Boaventura, Application of the Nernst–Planck approach to lead ion exchange in Ca-loaded *Pelvetia canaliculata*, Water Res., 44 (2010) 3946–3958.

[7] W.L. Ang, A.W. Mohammad, N. Hilal, C.P. Leo, A review on the applicability of integrated/hybrid membrane processes in water treatment and desalination plants, Desalination, 363 (2015) 2–18.

[8] C.I. Gherasim, G. Bourceanu, R. Olariu, C. Arsene, Removal of lead(II) from aqueous solutions by a polyvinyl-chloride inclusion membrane without added plasticizer, J. Membr. Sci., 377 (2011) 167–174.

[9] G. Martínez-Paredes, M.B. González-García, A. Costa-García, In situ electrochemical generation of gold nanostructured screen-printed carbon electrodes. Application to the detection of lead underpotential deposition, Electrochim. Acta, 54 (2009) 4801–4808.

[10] S.K.R. Yadanaparthi, D. Graybill, R. von Wandruszka, Adsorbents for the removal of arsenic, cadmium, and lead from contaminated waters, J. Hazard. Mater., 171 (2009) 1–15.

[11] A. Bée, D. Talbot, S. Abramson, V. Dupuis, Magnetic alginate beads for Pb(II) ions removal from wastewater, J. Colloid Interface Sci., 362 (2011) 486–492.

[12] P. Xu, G.M. Zeng, D.L. Huang, C.L. Feng, S. Hu, M.H. Zhao, C. Lai, Z. Wei, C. Huang, G.X. Xie, Z.F. Liu, Use of iron oxide nanomaterials in wastewater treatment: a review, Sci. Total Environ., 424 (2012) 1–10.

[13] S.S. Gupta, K.G. Bhattacharyya, Kinetics of adsorption of metal ions on inorganic materials: a review, Adv. Colloid Interface Sci., 162 (2011) 39–58.

[14] X.Y. Gu, J. Sun, L.J. Evans, The development of a multi-surface soil speciation model for Cd (II) and Pb (II): comparison of two approaches for metal adsorption to clay fractions, Appl. Geochem., 47 (2014) 99–108.

[15] M. Anari-Anaraki, A. Nezamzadeh-Ejhieh, Modification of an Iranian clinoptilolite nano-particles by hexadecyltrimethyl ammonium cationic surfactant and dithizone for removal of Pb(II) from aqueous solution, J. Colloid Interface Sci., 440 (2015) 272–281.

[16] D.G. Liu, Z.H. Li, Y. Zhu, Z.X. Li, R. Kumar, Recycled chitosan nanofibril as an effective Cu(II), Pb(II) and Cd(II) ionic chelating agent, adsorption and desorption performance, Carbohydr. Polym. J., 111 (2014) 469–476.

[17] W. Liu, Y.F. Liu, Y.Q. Tao, Y.J. Yu, H.M. Jiang, H.Z. Lian, Comparative study of adsorption of Pb(II) on native garlic peel and mercerized garlic peel, Environ. Sci. Pollut, Res., 21 (2014) 2054–2063.

[18] W.S.W. Ngah, M.A.K.M. Hanafiah, Removal of heavy metal ions from wastewater by chemically modified plant wastes as adsorbents: a review, Bioresour. Technol., 99 (2008) 3935–3948.

[19] Y. Huang, S.X. Li, J.H. Chen, X.L. Zhang, Y.P. Chen, Adsorption of Pb(II) on mesoporous activated carbons fabricated from water hyacinth using H$_3$PO$_4$ activation: adsorption capacity, kinetic and isotherm studies, Appl. Surf. Sci., 293 (2014) 160–168.

[20] X.L. Liang, Z. He, G.L. Wei, P. Liu, Y.H. Zhong, W. Tan, P.X. Du, J.X. Zhu, H.P. He, J. Zhang, The distinct effects of Mn substitution on the reactivity of magnetite in heterogeneous Fenton reaction and Pb(II) adsorption, J. Colloid Interface Sci., 426 (2014) 181–189.

[21] J. Zhang, S. Zhai, S. Li, Z. Xiao, Y. Song, Q. An, G. Tian, Pb(II) removal of Fe$_3$O$_4$@SiO$_2$–NH$_2$ core–shell nanomaterials prepared via a controllable sol–gel process, Chem. Eng. J., 215–216 (2013) 461–471.

[22] M.B. Jazi, M. Arshadi, M.J. Amiri, A. Gil, Kinetic and thermodynamic investigations of Pb(II) and Cd(II) adsorption on nanoscale organo-functionalized SiO$_2$-Al$_2$O$_3$, J. Colloid Interface Sci., 422 (2014) 16–22.

[23] A. Ngomsik, A. Bee, M. Draye, G. Cote, Valérie Cabuil, Magnetic nano- and microparticles for metal removal and environmental applications: a review, C. R. Chimie, 8 (2005) 963–970.

[24] H.T. Fan, X.T. Sun, Z.G. Zhang, W.X. Li, Selective removal of Lead(II) from aqueous solution by an ion-imprinted silica sorbent functionalized with chelating N-donor atoms, J. Chem. Eng. Data, 59 (2014) 2106–2114.

[25] D.P. Sui, H.X. Chen, L. Liu, M.X. Liu, C.C. Huang, H.T. Fan, Ion-imprinted silica adsorbent modified diffusive gradients in thin films technique: tool for speciation analysis of free lead species, Talanta, 148 (2016) 285–291.

[26] M. Shamsipur, H.R. Rajabi, S.M. Pourmortazavi, M. Roushani, Ion imprinted polymeric nanoparticles for selective separation and sensitive determination of zinc ions in different matrices, Spectrochim. Acta, Part A, 117 (2014) 24–33.

[27] M. Shamsipur, H.R. Rajabi, Flame photometric determination of cesium ion after its preconcentration with nanoparticles imprinted with the cesium-dibenzo-24-crown-8 complex, Microchim Acta, 180 (2013) 243–252.

[28] E. Turiel, A. Martín-Esteban, Molecularly imprinted polymers for sample preparation: a review, Anal. Chim. Acta, 668 (2010) 87–99.

[29] A. Beltran, F. Borrull, P.A.G. Cormack, R.M. Marcé, Molecularly-imprinted polymers: useful sorbents for selective extractions, Trends Anal. Chem., 29 (2010) 1363–1375.

[30] C. Li, J. Gao, J. Pan, Z. Zhang, Y. Yan, Synthesis, characterization, and adsorption performance of Pb(II)-imprinted polymer in nano-TiO$_2$ matrix, J. Environ. Sci., 21 (2009) 1722–1729.

[31] X. Zhu, Y. Cui, X. Chang, X. Zou, Z. Li, Selective solid-phase extraction of lead(II) from biological and natural water samples using surface-grafted lead(II)-imprinted polymers, Microchim. Acta, 164 (2009) 125–132.

[32] L. Wang, M. Zhou, Z. Jing, A. Zhong, Selective separation of lead from aqueous solution with a novel Pb(II) surface ion-imprinted sol-gel sorbent, Microchim. Acta, 165 (2009) 367–372.

[33] Y. Liu, Z. Liu, J. Gao, J. Dai, J. Han, Y. Wang, J. Xie, Y. Yan, Selective adsorption behavior of Pb(II) by mesoporous silica SBA-15-supported Pb(II)-imprinted polymer based on surface molecularly imprinting technique, J. Hazard. Mater., 186 (2011) 197–205.

[34] B. Guo, F. Deng, Y. Zhao, X. Luo, S. Luo, C. Au, Magnetic ion-imprinted and –SH functionalized polymer for selective removal of Pb(II) from aqueous samples, Appl. Surf. Sci., 292 (2014) 438–446.

[35] O. Sadeghi, F. Aboufazeli, H.R.L.Z. Zhad, M. Karimi, E. Najafi, Determination of Pb(II) ions using novel ion-imprinted polymer magnetic nanoparticles: investigation of the relation between Pb(II) ions in cow's milk and their nutrition, Food Anal. Methods, 6 (2013) 753–760.

[36] F. Aboufazeli, H.R.L.Z. Zhad, O. Sadeghi, M. Karimi, E. Najafi, Novel ion imprinted polymer magnetic mesoporous silica nano-particles for selective separation and determination of lead ions in food samples, Food Chem., 141 (2013) 3459–3465.

[37] O. Sayar, N.A. Torbati, H. Saravani, K. Mehrani, A. Behbahani, H.R.M. Zadeh, A novel magnetic ion imprinted polymer for selective adsorption of trace amounts of lead(II) ions in environment samples, J. Ind. Eng. Chem., 20 (2014) 2657–2662.

[38] H.T. Fan, Q. Tang, Y. Sun, Z.G. Zhang, W.X. Li, Selective removal of antimony(III) from aqueous solution using antimony(III)-imprinted organic–inorganic hybrid sorbents by combination of surface imprinting technique with sol–gel process, Chem. Eng. J., 258 (2014) 146–156.

[39] J.B. Wu, S.Y. Zang, Y.L. Yi, Sol-gel derived ion imprinted thiocyanato-functionalized silica gel as selective adsorbent of cadmium(II), J. Sol-Gel Sci. Technol., 66 (2013) 434–442.

[40] H.T. Fan, X.T. Sun, W.X. Li, Sol-gel derived ion-imprinted silica-supported organic-inorganic hybrid sorbent for selective removal of lead(II) from aqueous solution, J. Sol-Gel Sci. Technol., 72 (2014) 144–155.

[41] C. Sun, C. Zhang, C. Li, Y. Kuang, R. Qu, C. Ji, Y. Zhang, Syntheses of polyamine-bridged polysilsesquioxanes hybrid materials combining sol-gel processing and molecular imprinting applied to selective adsorption for copper, Mater. Chem. Phys., 153 (2015) 307–315.

[42] P.G. Su, F.C. Hung, P.H. Lin, Fabrication, characterization and sensing properties of Cu(II) ion imprinted sol-gel thin film on QCM, Mater. Chem. Phys., 135 (2012) 130–136.

[43] G. Wu, Z. Wang, J. Wang, C. He, Hierarchically imprinted organic–inorganic hybrid sorbent for selective separation of mercury ion from aqueous solution, Anal. Chim. Acta, 582 (2007) 304–310.

[44] H.R. Rajabi, S.R.H.R. Rajabi, S. Razmpour, Synthesis, characterization and application of ion imprinted polymeric nanobeads for highly selective preconcentration and spectrophotometric determination of Ni^{2+} ion in water samples, Spectrochim. Acta A, 153 (2016) 45–52.

[45] H.R. Rajabi, Z. Arezoo, K. Gholamreza, Porphyrin based nano-sized imprinted polymer as an efficient modifier for the design of a potentiometric copper carbon paste electrode, RSC Adv., 7 (2017)14923–14931.

[46] S.I. Lyubchik, A.I. Lyubchika O.L. Galushko, L.P. Tikhonova, J. Vital, I.M. Fonseca, S.B. Lyubchik, Kinetics and thermodynamics of the Cr(III) adsorption on the activated carbon from co-mingled wastes, Colloid. Surf. A, 242 (2004) 151–158.